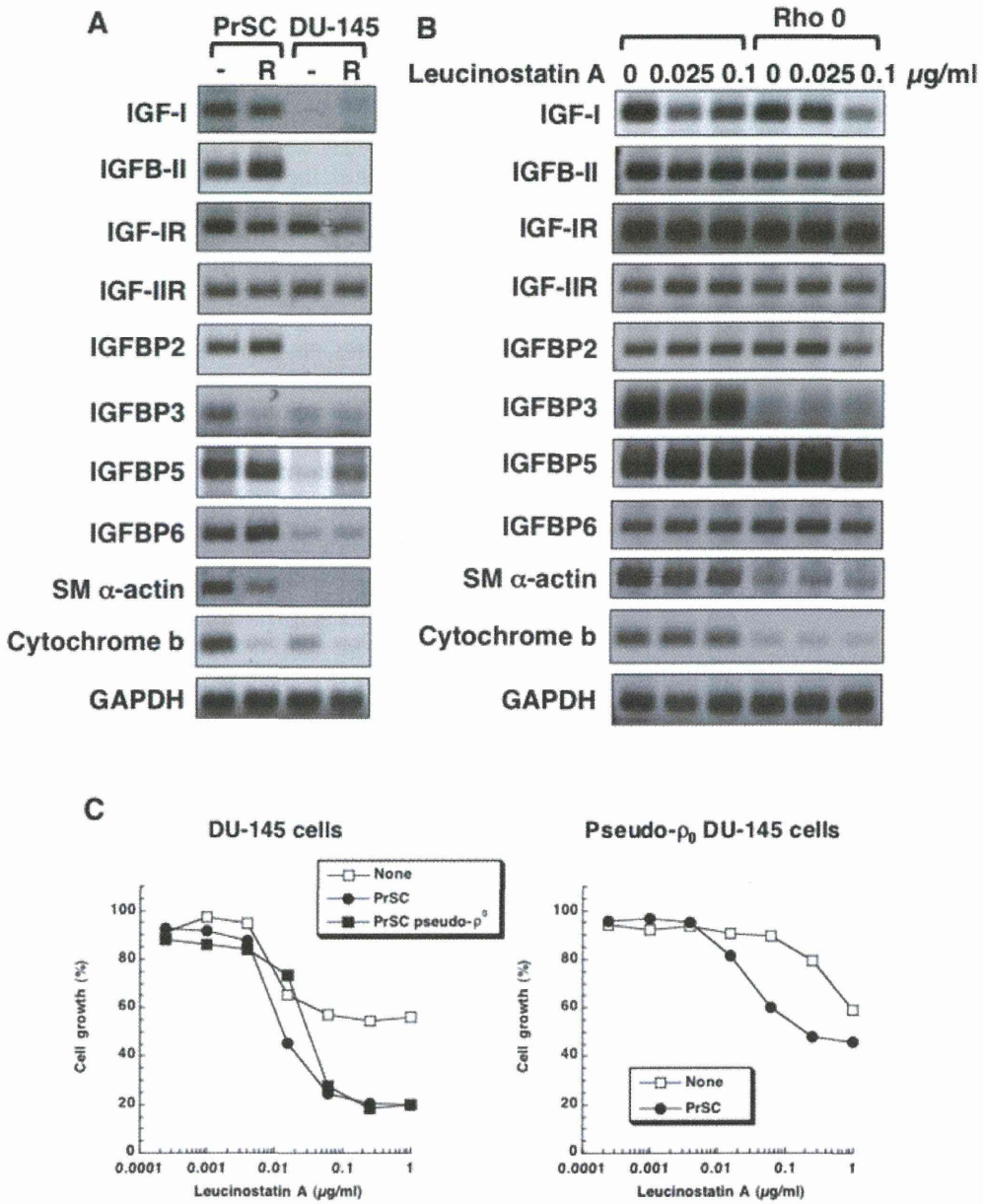

Figure 4. Effect of leucinostatin A on pseudo-ρ^0 cells. (*a*) PrSC and DU-145 cells were cultured with (R) or without (-) ethidium bromide. Total RNAs were collected and RT-PCR for the indicated molecules was carried out using specific primers. (*b*) PrSC or pseudo-ρ^0 PrSC (Rho0) were cultured with leucinostatin A for 2 days. Total RNAs were collected and RT-PCR for the indicated molecules was carried out using specific primers. (*c*) Effect of leucinostatin A on the growth of DU-145 cells (left) or pseudo-ρ^0 DU-145 cells (right) alone (open squares) or cocultured with PrSC (closed circles) or pseudo-ρ^0 PrSC (closed squares) was determined using rhodanile blue staining. Values are means of triplicate determinations [standard errors (SE) less than 10%].

of lecinostatins action was considered to be different from that of phthoxazolin A.

Leucinostatins are reported to inhibit oxidative phosphorylation in mitochondria[34] and atpenins are known as inhibitors of mitochondrial complex II.[29] There is a possibility that abrogation of mitochondrial functions could involve in the activity in our assay system. To examine the possible involvement of mitochondrial function in our assay system we employed pseudo-ρ^0 cells. Abrogation of mitochondrial functions resulted in reduction of the expression of SM α-actin

and IGFBP-3 in pseudo-ρ^0 PrSC, but it unexpectedly couldn't affect IGF-I expression (Fig. 4). Furthermore, leucinostatin A inhibited the growth of DU-145 cells cocultured with pseudo-ρ^0 PrSC more strongly than that in monoculture and decreased IGF-I expression even in pseudo-ρ^0 PrSC (Fig. 4). On the other hand, the growth inhibitory effect of leucinostatin A was apparently weakened against pseudo-ρ^0 DU-145 cells, but the growth of pseudo-ρ^0 DU-145 cells in coculture with PrSC was inhibited more strongly than that in monoculture by leucinostatin A (Fig. 4). These results indicated that one of leucinostatin action was actually inhibition of mitochondrial function. This result correlated well with the partial recovery of leucinostatin A-inuduced growth inhibition by the external IGF-I (Supporting Information Fig. 3). However, there is certainly another mechanism for the inhibition of IGF-I expression, which brought about the inhibition of growth of DU-145 cells in coculture with PrSC. It is reported that c-jun upregulates IGF-I production in prostate stroma.[37] We examined the effect of leucinostatin A on c-jun expression in PrSC, but found no change in response to leucinostatin A (Supporting Information Fig. 3).

To extrapolate the *in vitro* finding to *in vivo*, we examined whether leucinostatin A reduces IGF-I expression in the tumor tissues. Our preliminary results revealed that DU-145 tumor tissues contained significant amounts of SM α-actin positive cells and IGF-I staining due to the coinoculation of PrSC, but leucinostatin A treatment reduced the IGF-I staining without effect on the amounts of SM α-actin positive cells (Supporting Information Figure 4). Although more precise studies must be needed, this result correlates well with the *in vitro* result.

Because leucinostatin A inhibited the growth of DU-145 tumors in the presence of PrSC, we have tried to evaluate its antitumor effect against orthotopic model of prostate tumors. When we examined the effect of leucinostatin A on orthotopic implanted DU-145 xenograft in mice, we found that leucinostatin A inhibited metastases of DU-145 tumors. Our preliminary results showed that leucinostatin A unfortunately failed to inhibit the growth of primary tumors in the mouse prostate, but it possibly suppressed the metastases of DU-145 tumors. DU-145 tumors formed diaphragmatic metastases (4 mice out of 6 mice, 67%) and peritoneal metastases (5 out of 6, 83%) (Supporting Information Fig. 5), but leucinostatin A treatment reduced the metastases as diaphragmatic metastases (1 out of 3, 33%) and peritoneal metastases (0 out of 3, 0%). Although further evaluation must be needed for the orthotopic model of prostate tumors, there is a possibility that modulators of tumor-stromal cell interactions could apply for antimetastases of tumors.

In summary our results showed that leucinostatin A abrogated tumor-stromal cell interactions through inhibition of IGF-I expression from PrSC and inhibited the growth of prostate cancer cells *in vitro* and *in vivo*. Although the precise mechanism of leucinostatin A on inhibition of IGF-I expression in PrSC is needed further study, our results clearly promote the notion that small molecule modulators of tumor-stromal cell interactions can suppress tumor growth *in vivo*. We are now continuing to search for more potent compounds in our assay system.

Acknowledgements

The authors are grateful to Meiji Seika Kaisha, Ltd. for fermentation broths of fungal strains and Dr. Y. Takahashi, Dr. T. Shitara, Ms. I. Kurata, Dr. T. Someno, Dr. M. Arakawa, Ms. K. Adachi, and Ms. E. Satoh for their technical assistance.

Fast Track

References

1. Stahtea XN, Roussidis AE, Kanakis I, Tzanakakis GN, Chalkiadakis G, Mavroudis D, Kletsas D, Karamanos NK. Imatinib inhibits colorectal cancer cell growth and suppresses stromal-induced growth stimulation. MT1-MMP expression and pro-MMP2 activation. *Int J Cancer* 2007;121:2808–14.
2. Wiseman BS, Werb Z. Stromal effects on mammary gland development and breast cancer. *Science* 2002;296:1046–9.
3. Karnoub AE, Dash AB, Vo AP, Sullivan A, Brooks MW, Bell GW, Richardson AL, Polyak K, Tubo R, Weinberg RA. Mesenchymal stem cells within tumour stroma promote breast cancer metastasis. *Nature* 2007;449:557–63.
4. Hwang RF, Moore T, Arumugam T, Ramachandran V, Amos KD, Rivera A, Ji B, Evans DB, Logsdon CD. Cancer-associated stromal fibroblasts promote pancreatic tumor progression. *Cancer Res* 2008;68:918–26.
5. Grossfeld GD, Hayward SW, Tlsty TD, Cunha GR. The role of stroma in prostatic carcinogenesis. *Endocr Relat Cancer* 1998;5: 253–70.
6. Tuxhorn JA, Ayala GE, Smith MJ, Smith VC, Dang TD, Rowley DR. Reactive stroma in human prostate cancer: induction of myofibroblast phenotype and extracellular matrix remodeling. *Clin Cancer Res* 2002;8: 2912–23.
7. Dvorak HF. Tumors: wounds that do not heal. Similarities between tumor stroma generation and wound healing. *N Engl J Med* 1986;315:1650–9.
8. Delinassios JG. Cytocidal effects of human fibroblasts on HeLa cells in vitro. *Biol Cell* 1987;59:69–77.
9. Picard O, Rolland Y, Poupon MF. Fibroblast-dependent tumorigenicity of cells in nude mice: implication for implantation of metastases. *Cancer Res* 1986;46:3290–4.
10. Camps JL, Chang SM, Hsu TC, Freeman MR, Hong SJ, Zhau HE, von Eschenbach AC, Chung LW. Fibroblast-mediated acceleration of human epithelial tumor growth *in vivo*. *Proc Natl Acad Sci USA* 1990;87:75–9.
11. Micke P, Ostman A. Tumour-stroma interaction: cancer-associated fibroblasts as novel targets in anti-cancer therapy? *Lung Cancer* 2004;45 (Suppl 2):S163–S175.
12. Tuxhorn JA, Ayala GE, Rowley DR. Reactive stroma in prostate cancer progression. *J Urol* 2001;166:2472–83.
13. Wernert N. The multiple roles of tumour stroma. *Virchows Arch* 1997;430:433–43.
14. Kawada M, Inoue H, Masuda T, Ikeda D. Insulin-like growth factor I secreted from prostate stromal cells mediates tumor-stromal cell interactions of prostate cancer. *Cancer Res* 2006;66:4419–25.
15. Pollak M, Beamer W, Zhang JC. Insulin-like growth factors and prostate cancer. *Cancer Metastasis Rev* 1998;17:383–90.

16. Kiaris H, Trimis G, Papavassiliou AG. Regulation of tumor-stromal fibroblast interactions: implications in anticancer therapy. *Curr Med Chem* 2008;15: 3062–7.
17. Tsellou E, Kiaris H. Fibroblast independency in tumors: implications in cancer therapy. *Future Oncol* 2008;4: 427–32.
18. Date K, Matsumoto K, Kuba K, Shimura H, Tanaka M, Nakamura T. Inhibition of tumor growth and invasion by a four-kringle antagonist (HGF/NK4) for hepatocyte growth factor. *Oncogene* 1998; 17:3045–54.
19. Kawada M, Ishizuka M, Takeuchi T. Enhancement of antiproliferative effects of interleukin-1β and tumor necrosis factor-α on human prostate cancer LNCaP cells by coculture with normal fibroblasts through secreted interleukin-6. *Jpn J Cancer Res* 1999;90:546–54.
20. Tuxhorn JA, McAlhany SJ, Yang F, Dang TD, Rowley DR. Inhibition of transforming growth factor-β activity decreases angiogenesis in a human prostate cancer-reactive stroma xenograft model. *Cancer Res* 2002;62:6021–5.
21. Kawada M, Yoshimoto Y, Minamiguchi K, Kumagai H, Someno T, Masuda T, Ishizuka M, Ikeda D. A microplate assay for selective measurement of growth of epithelial tumor cells in direct coculture with stromal cells. *Anticancer Res* 2004;24: 1561–8.
22. Kawada M, Inoue H, Usami I, Ikeda D. Phthoxazolin A inhibits prostate cancer growth by modulating tumor-stromal cell interactions. *Cancer Sci* 2009;100:150–7.
23. Kawada M, Momose I, Someno T, Tsujiuchi G, Ikeda D. New atpenins, NBRI23477 A and B, inhibit the growth of human prostate cancer cells. *J Antibiot* 2009;62:243–6.
24. Kent RJ, Norris DE. Identification of mammalian blood meals in mosquitoes by a multiplexed polymerase chain reaction targeting cytochrome B. *Am J Trop Med Hyg* 2005;73:336–42.
25. Kawada M, Masuda T, Ishizuka M, Takeuchi T. 15-Deoxyspergualin inhibits Akt kinase activation and phosphatidylcholine synthesis. *J Biol Chem* 2002;277:27765–71.
26. Tartier L, Gilchrist S, Burdak-Rothkamm S, Folkard M, Prise KM. Cytoplasmic irradiation induces mitochondrial-dependent 53BP1 protein relocalization in irradiated and bystander cells. *Cancer Res* 2007;67:5872–9.
27. Omura S, Tomoda H, Kimura K, Zhen DZ, Kumagai H, Igarashi K, Imamura N, Takahashi Y, Tanaka Y, Iwai Y. Atpenins, new antifungal antibiotics produced by *Penicillium sp.* Production, isolation, physico-chemical and biological properties. *J Antibiot* 1988;41:1769–73.
28. Kumagai H, Nishida H, Imamura N, Tomoda H, Omura S, Bordner J. The structures of atpenins A4. A5 and. B, new antifungal antibiotics produced by *Penicillium sp. J Antibiot.* 1990;43:1553–8.
29. Miyadera H, Shiomi K, Ui H, Yamaguchi Y, Masuma R, Tomoda H, Miyoshi H, Osanai A, Kita K, Omura S. Atpenins, potent and specific inhibitors of mitochondrial complex II (succinate-ubiquinone oxidoreductase). *Proc Natl Acad Sci USA* 2003;100:473–7.
30. Arai T, Mikami Y, Fukushima K, Utsumi T, Yazawa K. A new antibiotic, leucinostatin, derived from *Penicillium lilacinum.*. *J Antibiot* 1973;26:157–61.
31. Fukushima K, Arai T, Mori Y, Tsuboi M, Suzuki M. Studies on peptide antibiotics, leucinostatins. I. Separation, physico-chemical properties and biological activities of leucinostatins A and B. *J Antibiot* 1983; 36:1606–12.
32. Fukushima K, Arai T, Mori Y, Tsuboi M, Suzuki M. Studies on peptide antibiotics, leucinostatins. II. The structures of leucinostatins A and B. *J Antibiot* 1983;36: 1613–30.
33. Kawada M, Inoue H, Arakawa M, Ikeda D. Transforming growth factor-β1 modulates tumor-stromal cell interactions of prostate cancer through insulin-like growth factor-I. *Anticancer Res* 2008;28:721–30.
34. Shima A, Fukushima K, Arai T, Terada H. Dual inhibitory effects of the peptide antibiotics leucinostatins on oxidative phosphorylation in mitochondria. *Cell Struct Funct* 1990;15:53–8.
35. Lafkas D, Trimis G, Papavassiliou AG, Kiaris H. P53 mutations in stromal fibroblasts sensitize tumors against chemotherapy. *Int J Cancer* 2008;123: 967–71.
36. Bromfield GP, Meng A, Warde P, Bristow RG. Cell death in irradiated prostate epithelial cells: role of apoptotic and clonogenic cell kill. *Prostate Cancer Prostatic Dis* 2003;6:73–85.
37. Li W, Wu CL, Febbo PG, Olumi AF. Stromally expressed c-Jun regulates proliferation of prostate epithelial cells. *Am J Pathol* 2007;171:1189–98.

Fast Track

Biosci. Biotechnol. Biochem., **74** (9), 1913–1919, 2010

Increased ABCB1 Expression in TP-110-Resistant RPMI-8226 Cells

Masatomi IIJIMA,† Isao MOMOSE, and Daishiro IKEDA

Numazu Bio-Medical Research Institute, Microbial Chemistry Research Center, 18-24 Miyamoto, Numazu, Shizuoka 410-0301, Japan

Received April 27, 2010; Accepted June 11, 2010; Online Publication, September 7, 2010
[doi:10.1271/bbb.100325]

TP-110, a novel proteasome inhibitor, has been found to possess potent growth inhibition in human multiple myeloma cells. To enhance its therapeutic effects, we established TP-110-resistant RPMI-8226 (RPMI-8226/TP-110) cells and elucidated their resistance mechanisms. The IC_{50} value for TP-110 cytotoxicity in the RPMI-8226/TP-110 cells was about 10-fold higher than that of the parental sensitive cells. The RPMI-8226/TP-110 cells exhibited distinct drug resistance to other proteasome inhibitors. Furthermore, they showed high cross-resistance to the cytotoxic effects of doxorubicin, etoposide, taxol, and vincristine. P-glycoprotein (MDR1), encoded by *ABCB1*, was elevated in the RPMI-8226/TP-110 cells, and the MDR1 inhibitor verapamil overcame their resistance to TP-110. The results of DNA microarray and RT-PCR suggested that the expression of ABCB1 is significantly elevated in RPMI-8226/TP-110 cells. This indicates that resistance in RPMI-8226/TP-110 cells is involved in the expression of P-glycoprotein, a drug-efflux pump.

Key words: proteasome inhibitor; ABCB1; TP-110

The ubiquitin-proteasome system is involved in the cell cycle, signal transduction, the cellular stress response, and the immune response.[1] Because cancer cells are more highly proliferative than normal cells, their protein translation and degradation is also higher.[2] Accordingly, inhibitors of the proteasome represent a promising group of chemotherapeutic agents for cancer treatment.

Previous research has demonstrated that MG-132, lactacystin, and bortezomib have proteasome inhibitory activities.[3–5] Bortezomib, a dipeptide boronic acid, shows significant anti-tumor activity in multiple myeloma cells. In 2003, the U.S. Food and Drug Administration (FDA) approved bortezomib (VELCADE™), formerly known as PS-341, for the treatment of relapsed/refractory multiple myeloma.[6]

We have reported the isolation of a new proteasome inhibitor, tyropeptin A, produced by *Kitasatospora* sp. MK993-dF2.[7–10] In an effort to enhance its inhibitory potency, a structural model of tyropeptin A bound to the site responsible for chymotrypsin-like activity of the mammalian 20S proteasome was constructed. Based on these modeling experiments, several derivatives were synthesized. One of them, TP-110, specifically inhibits chymotrypsin-like activity, but does not inhibit the post-glutamyl-peptide hydrolyzing (PGPH) and trypsin-like activities of the 20S proteasome.[11] TP-110 strongly inhibits the growth of human tumor cells and induces apoptosis.[12] One of the mechanisms of apoptosis induction by TP-110 is down-regulation of inhibitors of apoptosis proteins (IAPs) in multiple myeloma cells.[13]

A loss of anti-tumor efficacy responsible for drug-resistance in cells is known in cancer chemotherapy. ABC (ATP binding cassette) transporters are well-known multi-drug efflux transporters that depend on ATP.[14] One of these, ABCB1 (MDR1), is a representative transporter involved in human multi-drug resistant tumor cells. In addition to ABCB1, expression of ABCC1 (MRP1) and ABCG2 (BCRP) has also been found in tumor cell lines.[15–17] To overcome multi-drug resistance (MDR), MDR inhibitors have been developed. Verapamil, cyclosporin A and tamoxifen are first-generation MDR inhibitors,[18] and the next generation of inhibitors and antibodies for MDR are now being studied.[19] These inhibitors or antibodies might significantly contribute to overcoming anticancer drug resistance.

We have been developing novel proteasome inhibitors as candidate anti-tumor agents. To strengthen their therapeutic effects, we have also been investigating methods of overcoming resistance. Here we report the involvement of ABCB1 in the resistance mechanisms of RPMI-8226/TP-110 cells.

Materials and Methods

Chemicals and antibodies. TP-110, a tyropeptin A derivative, was synthesized at the Numazu Bio-Medical Research Institute, Numazu, Japan.[9] It was dissolved in DMSO (10 mg/ml), stored at −20 °C, and diluted with PBS (pH 7.4). The chemical structure of TP-110 is shown in Fig. 1. MG-132 and lactacystin were purchased from the Peptide Institute (Osaka, Japan). Bortezomib was synthesized at the Microbial Chemistry Research Institute (Tokyo, Japan). Anti-cancer drugs were purchased from Sigma (St. Louis, MO). Antibodies were obtained as follows: rabbit anti-caspase-3 (sc-7148) and rabbit anti-mdr (sc-8313) (Santa Cruz Biotechnology, Santa Cruz, CA); mouse anti-cytochrome *c* (7H8.2C12) (BD BioScience, San Diego); mouse anti-α-tubulin (B-5-1-2) (Sigma); and mouse anti-mrp1 (QCRL-1) (Chemicon International, Temecula, CA).

Cells and establishment of TP-110-resistant cells. Human multiple myeloma RPMI-8226 cells were purchased from ATCC. Initial induction of resistant cells were achieved by continuous exposure of RPMI-8226 cells to TP-110 (10 ng/ml) over 3 months. Growing resistant cells were further treated with gradually increasing concen-

† To whom correspondence should be addressed. Fax: +81-55-922-6888; E-mail: iijimam@bikaken.or.jp
Abbreviations: ABC, ATP binding cassette; MDR, multidrug resistance; P-gp, P-glycoprotein; IAPs, intrinsic inhibitor of apoptosis proteins

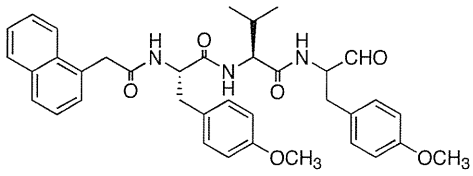

Fig. 1. Structure of TP-110.

trations of TP-110 (up to a final concentration of 100 ng/ml for RPMI-8226 cells). The resistant RPMI-8226 cells that survived exposure to TP-110 (100 ng/ml) were cloned by the limiting dilution method. Chronic leukemia K-562 cells and doxorubicin-resistant K-562 (K-562/DOX) cells were provided by Dr. Setsuko Kunimoto at our laboratory. Cells were grown in RPMI1640 medium supplemented with 10% FBS, 100 U/ml of penicillin G, and 100 μg/ml of streptomycin at 37 °C with 5% CO_2.

Proteasome activity. The chymotrypsin-like activity of the 20S proteasome was measured using a fluorogenic substance, as described previously.[7] The 20S proteasome was prepared from RPMI-8226 and RPMI-8226/TP-110 cells.

Cytotoxicity. Cells (1×10^4) were cultured in 96-well plates with a test sample. Cells from 72 h culture were pulsed with MTT (3-(4,5-dimethyl-2-thiazolyl)-2,5-diphenyl-2H-tetrazolium bromide) for 4 h, and were incubated in the presence of 10% SDS for 20 h. Absorbance was measured at 570 nm using a spectrophotometer (Dainippon Sumitomo Pharma, Osaka, Japan).

Cell cycle analysis. Cells (1×10^4) were cultured with and without 0.1 μg/ml TP-110 for 24 h. Cells fixed using 70% ethanol were treated with 0.1% RNase A at 37 °C for 15 min, and were then incubated with propidium iodide (PI). DNA fluorescence was analyzed using a fluorescence-activated cell sorter (FACSCalibur; BD Bioscience, Franklin Lakes, NJ).

Caspase-3 activity. Cells (5×10^5) were cultured with TP-110 for 24 h, washed twice with PBS, and lysed in cell extraction buffer containing 50 mM HEPES (pH 7.4), 5 mM CHAPS, and 5 mM DTT, and were stored at −80 °C. Cell extracts were centrifuged at 14,000 × *g* for 10 min at 4 °C, and the caspase-3 activity of the supernatant was assessed with a caspase-3 assay kit (Sigma). This assay is based on the hydrolysis of a peptide substrate, acetyl-Asp-Glu-Val-Asp-7-amino-4-methylcoumarin (Ac-DEVD-AMC), by caspase-3. After incubation at 37 °C for 30 min, fluorescence intensity (excitation and emission wavelengths of Ac-DEVD-AMC, 380 nm and 460 nm respectively) was measured with Fluoroskan II (Dainippon Sumitomo Pharma, Osaka, Japan).

Western blot analysis. Cultured cells were harvested, washed twice with PBS, and suspended in lysis buffer containing 20 mM HEPES (pH 7.5), 150 mM NaCl, 1% Triton X-100, 10% glycerol, 1 mM EDTA, 50 mM NaF, 50 mM β-glycerophosphate, 1 mM Na_3VO_4, 25 μg/ml of antipain, 25 μg/ml of leupeptin and 25 μg/ml of pepstatin at 4 °C for 15 min. After centrifugation at 15,000 rpm, the supernatant was assessed using a Bio-Rad protein assay kit (Bio-Rad, Hercules, CA). The cytosol fraction was extracted at 4 °C for 5 min using digitonin lysis buffer containing 10 mM HEPES, 0.3 M mannitol 0.1% BSA, and 0.1 mM digitonin, and centrifuged at 8,500 × *g* for 5 min at 4 °C. Equal amounts of the protein extract were subjected to SDS–PAGE. The isolated protein was then transferred onto an Immobion PVDF membrane (Millipore, Bedford, MA). The membrane was blocked with 5% non-fat milk in Tris-buffered saline containing 0.1% Tween 20 (TBS-T) for 60 min. After washing with TBS-T, the membrane was incubated with primary antibody in blocking solution for 60 min at room temperature. After further washing with TBS-T, the membrane was then incubated with secondary antibody (anti-rabbit or anti-mouse immunoglobulin-horseradish peroxidase) for 30 min. The protein detected was visualized by the enhanced chemiluminescence reaction (ECL) procedure (GE Healthcare UK, Chalfont, UK).

Table 1. Growth Inhibitory Activity of TP-110 on Established Clones of RPMI-8226 Cells

		IC_{50} (μg/ml)	Index of resistance
RPMI-8226		0.020	1
RPMI-8226/TP-110	Clone 1	0.26	13
	Clone 2	0.18	9
	Clone 3	0.40	20
	Clone 4	0.31	16
	Clone 5	0.39	20
	Clone 6	0.45	23
	Clone 7	0.46	23
	Clone 8	0.47	24
	Clone 9	0.43	22
	Clone 10	0.25	13

RT-PCR analysis. Total RNA was isolated from the cells using an RNeasy Kit (Qiagen, Valencia, CA). cDNA was prepared from total RNA using a Reverse Transcription System (Promega, Madison, WI). PCR was conducted using Promega PCR Master Mix (Promega) and a pair of specific primers. The primers used were as follows: *ABCB1*-sense 5′-AGAGGATCGCCATTGCGCGT-3′ and *ABCB1*-antisense 5′-CCTGCTGTCTGCATTGTGAC-3′; *ABCC1*-sense AGTGACCTC-TGGTCCTTAAACAAGG-3′ and *ABCC1*-antisense GAGGTAGAG-AGCAAGGTAGACTTGC-3′; and *GAPDH*-sense 5′-GATGACATC-AAGAAGGTGGTGAA-3′ and *GAPDH*-antisense 5′-GTCTTACTCC-TTGGAGGCCTAGT-3′. The PCR products were electrophoresed on 2% agarose gels, and were detected by SYBR Green I nucleic acid gel staining (Molecular Probes, Eugene, OR).

cDNA microarray analysis. Labeled antisense RNA was prepared from the total RNA of the cells using of an RNA Transcript Sure LABEL Core Kit (Takara Bio, Ohtsu, Japan) with Cy3- and Cy5-dUTP (GE Healthcare, Piscataway, NJ). The cDNA microarray system used the IntelliGene HS Human Expression CHIP, which contains 16,600 spots of cDNA sequences. Microarrays were scanned using a 428-Array Scanner (Affymetrix, Santa Clara, CA).

Results

Establishment of RPMI-8226/TP-110 cells

RPMI-8226/TP-110 cells were developed over a 9-month period by continuous stepwise exposure to increasing concentrations of TP-110, and 10 clones were isolated by the limiting dilution method. The IC_{50} value for TP-110 cytotoxicity in the RPMI-8226/TP-110 cells showed a 9 to 24-fold increase as compared to the parental sensitive cells. Among these, we selected three strains (clone 2, clone 5, and clone 7), that exhibited distinct indices of resistance (Table 1).

Characteristics of the RPMI-8226/TP-110 cells

The morphology of RPMI-8226/TP-110 cells did not change as compared to the parent cells. Although the endogenous proteasome activities of RPMI-8226/TP-110 increased 1.4 to 1.6 fold, the sensitivity of the proteasome to TP-110 in the RPMI-8226/TP-110 cells were similar to that of the parent cells (Fig. 2A and B). Previous studies have indicated that TP-110 induced apoptosis in RPMI-8226 cells at 12 nM.[11] The effects of TP-110 on the cell cycle of the parent and the resistant cells are shown in Fig. 3A. Treatment with TP-110 for 24 h increased the number of cells in sub-G_1 and decreased the number of cells in G_1 and G_2M on the parent sensitive cells. However, the RPMI-8226/TP-110 cells were tolerant of TP-110 (Fig. 3A). Similarly, the

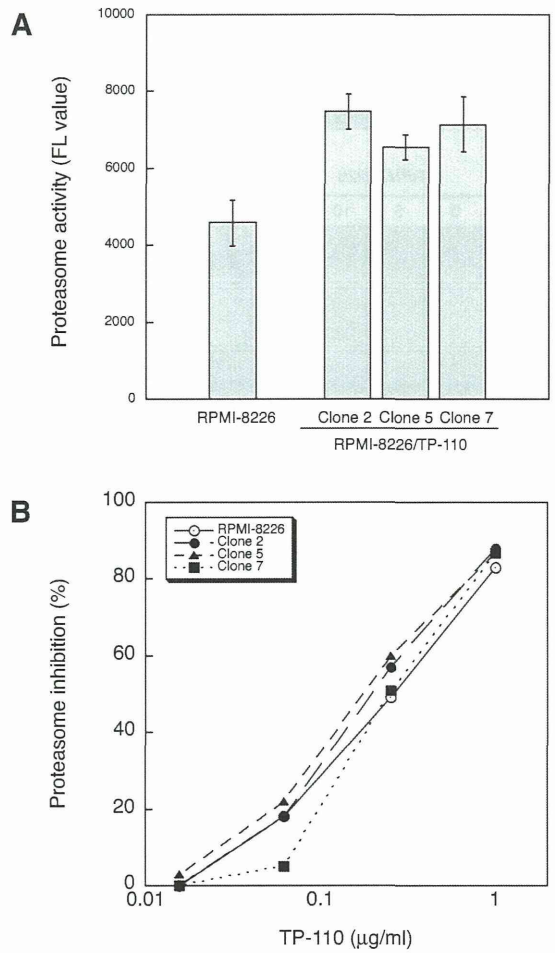

Fig. 2. Proteasome Activity in RPMI-8226/TP-110 Cells.
A, Protein extracts from 1×10^5 cells were assessed. The chymotrypsin-like activity of 20S proteasome was measured as described in "Materials and Methods." B, Inhibition of 20S proteasome by TP-110 in established resistant cells. TP-110 was added to the various enzyme reaction mixture.

addition of TP-110 to the parent sensitive cells strongly released cytochrome *c* into the cytosol, induced the active form of caspase-3, and increased caspase-3 activity, but the addition of TP-110 to RPMI-8226/TP-110 cells did not produce similar results (Fig. 3B, C, and D). This suggests that RPMI-8226/TP-110 cells are tolerant TP-110.

Cross-resistance pattern of RPMI-8226/TP-110 cells

Drug-resistant cells often exhibit cross-resistance to other drugs. First, we examined the cross-resistance to other proteasome inhibitors of RPMI-8226/TP-110 cells. The RPMI-8226/TP-110 cells showed cross-resistance to MG-132 (2.9 to 3.5 fold) and bortezomib (1.4 to 2.1 fold), but these cells showed no cross-resistance to lactacystin. Second, the cross-resistance to several anticancer drugs of RPMI-8226/TP-110 cells was examined. The RPMI-8226/TP-110 cells were also cross-resistant to DNA-interacting drugs, mitosis blocking drugs, topo II inhibitors, and anti-metabolite drugs. In particular, they showed potent cross-resistance to doxorubicin (40 to 115 fold), taxol (375 to 500 fold), vincristine (212 to 253 fold), and etoposide (202 to 396 fold) (Table 2).

Table 2. Cytotoxic Effects of Proteasome Inhibitors and Antitumor Agents on RPMI-8226/TP-110 Cells

Compound	IC_{50} (μg/ml)			
	RPMI-8226	RPMI-8226/TP-110		
		Clone 2	Clone 5	Clone 7
TP-110	0.030	0.37 (12*)	0.34 (11)	0.21 (7.0)
MG-132	0.48	1.4 (2.9)	1.7 (3.5)	1.6 (3.3)
Bortezomib	0.0018	0.0025 (1.4)	0.0037 (2.1)	0.0031 (1.7)
Lactacystin	1.0	0.71 (0.70)	0.53 (0.53)	0.76 (0.76)
Doxorubicin	0.0080	0.32 (40)	0.92 (115)	0.84 (114)
Mitomycin C	0.16	0.42 (2.6)	0.54 (3.4)	0.77 (4.8)
Actinomycin D	0.0074	0.18 (24)	0.33 (44)	0.45 (61)
Taxol	0.0080	3.1 (388)	4.0 (500)	3.0 (375)
Vincristine	0.0017	0.43 (253)	0.36 (212)	0.42 (247)
Vinblastine	0.0078	0.17 (22)	0.14 (18)	0.19 (24)
Etoposide	0.048	9.7 (202)	19 (396)	17 (354)
5-Fluorouracil	0.24	0.66 (2.8)	0.17 (0.71)	0.44 (1.8)

*Values in parentheses indicate index of resistance (fold).

DNA microarray analysis

DNA microarray analysis is informative in elucidating the mechanisms of drug action. Parent RPMI-8226 cells and RPMI-8226/TP-110 cells were incubated in fresh medium for 24 h, and total RNA was then extracted from the control (parent) and the experimental (resistant) cells. The changes in mRNA expression in the RPMI-8226/TP-110 cells are shown in Table 3. *ABCB1*, *FLJ10178*, *HSPB8*, *CCL2*, *AUTS2*, *RPIB9*, *ZNF521*, *CYP24A1*, *CFC1*, and *BTBD3* showed increased expression in the resistant cells, while *FN1*, *SLC27A2*, *TOM1L1*, *EPDR1*, *CADPS2*, *KIAA0802*, *STARD3NL*, *HMGA2*, *FLJ14564*, and *DMRT2* showed decreased expression. Among those genes showing altered expression, *ABCB1* is known to be involved in MDR. The expression levels of 44 ABC transporter genes are shown in Table 4. Among the ABC transporters examined, only *ABCB1* showed higher expression. This suggests that the ABCB1 transporter is profoundly involved in the mechanism of drug resistance in RPMI-8226/TP-110 cells.

Expression of ABCB1 in RPMI-8226/TP-110 cells

Expression of ABCB1 in the RPMI-8226/TP-110 cells was confirmed by RT-PCR and Western blotting. ABCB1 expression was markedly elevated in these cells, but the expression of ABCC1 (MRP1) was not elevated as to mRNA and protein levels (Fig. 4A and B).

Effects of ABC transporter inhibitors on RPMI-8226/TP-110 cells

In order to determine whether the ABCB1 transporter is involved in the resistance mechanism in the RPMI-8226/TP-110 cells, we examined the effects of an ABC transporter inhibitor. The addition of verapamil, well-known to be an ABC transporter antagonist, reversed not only TP-110 resistance, but also the MG-132, bortezomib, and doxorubicin resistance in the RPMI-8226/TP-110 cells (Table 5). Additionally, we examined the effects of other MDR1 inhibitors and other a Ca^{2+} antagonists, because verapamil has the effect of a Ca^{2+} antagonist. In results, MDR1 inhibitors (cyclosporin A and qunidine) reversed TP-110 resistance, but Ca^{2+}

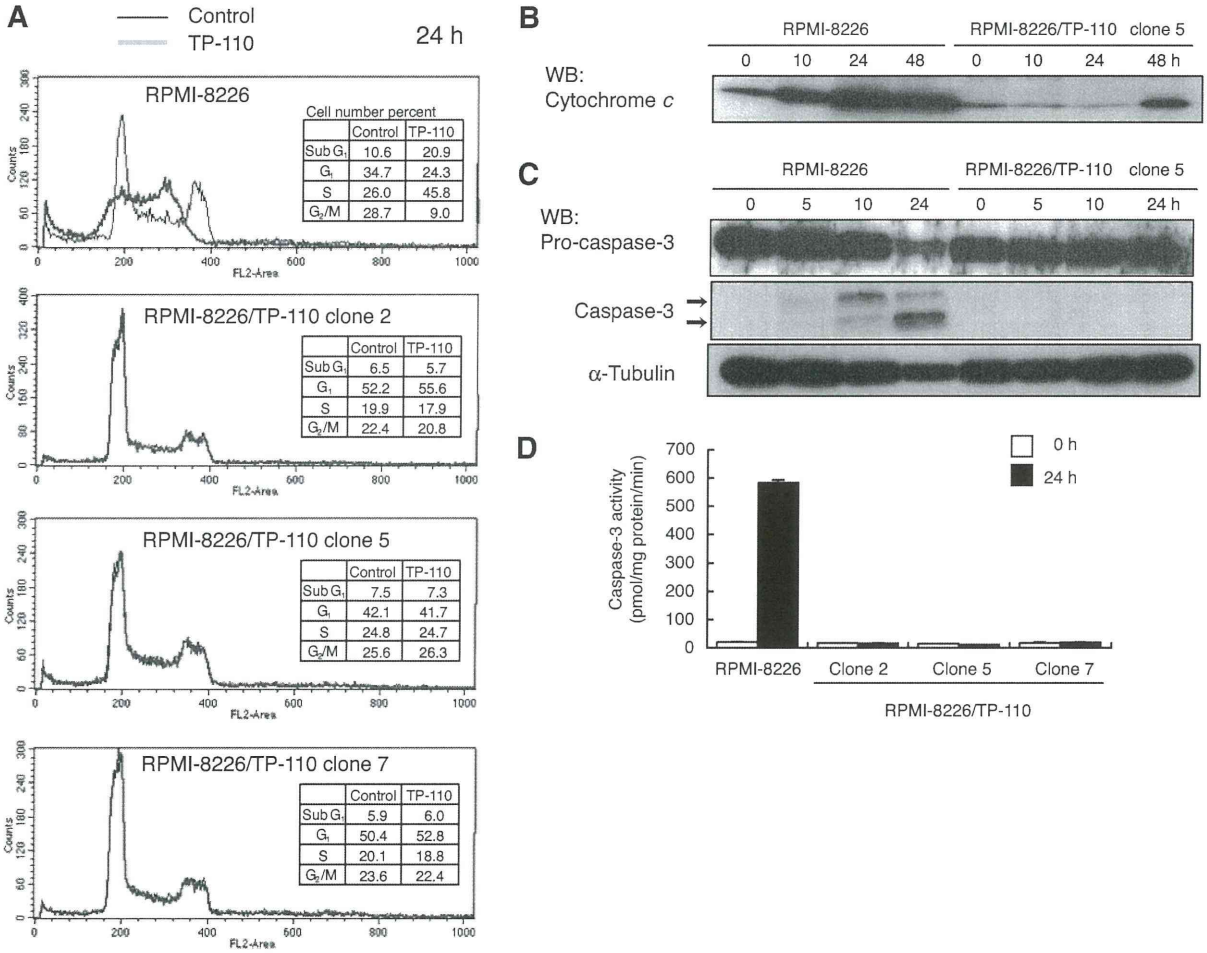

Fig. 3. Characteristics of the RPMI-8226/TP-110 Cells.

Cells were incubated with 0.1 μg/ml TP-110. A, After 24 h, the cells were examined by flow cytometry. B, Cells were incubated with 0.1 μg/ml TP-110. After 10, 24, and 48 h, the cytosol fraction of the cells was extracted using digitonin lysis buffer. C, After 24 h, Western blot analysis was performed using whole cell lysates, as described in "Materials and Methods." D, After 24 h, the caspase-3 activity of whole-cell lysates was assessed as described in "Materials and Methods."

antagonists (diltiazem and nifedipine) did not (Supplemental Table 1; see *Biosci. Biotechnol. Biochem.* Web site). This suggests that resistance in RPMI-8226/TP-110 cells depends on the expression of ABCB1.

Effects of TP-110 on the K-562/DOX cells

Resistance to TP-110 in another cell line that expresses ABCB1 was then investigated. K-562/DOX cells showed high expression of ABCB1, but K-562 (parent) cells did not (Supplemental Fig. 1; see *Biosci. Biotechnol. Biochem.* Web site). Predictably, the K-562/DOX cells showed strong resistance to TP-110. With regard to other proteasome inhibitors, K-562/DOX cells showed resistance to MG-132 and bortezomib, similarly to the RPMI-8226/TP-110 cells, while they were not resistant to lactacystin (Tables 2 and 6).

Discussion

In cancer drug discovery, the proteasome is a promising molecular target.[5] In addition to the treatment of relapsed or refractory multiple myeloma, bortezomib is also undergoing clinical trials for the treatment of several cancers (*e.g.*, prostate).[20] TP-110 (Fig. 1) strongly inhibits the growth of various human cell lines and induces apoptosis in their cells.[12] In order to strengthen its therapeutic effects, we established RPMI-8226/TP-110 cells and elucidated their resistance mechanisms.

Our results suggest that the factor involved in resistance of the RPMI-8226/TP-110 cells is *ABCB1*. DNA microarray is a useful tool to estimate changes in gene expression in cells. Our analytical results indicate that *ABCB1* is overexpressed in RPMI-8226/TP-110 cells (Table 3). The results of Western blotting and RT-PCR support the results of DNA microarray analysis. The addition of verapamil (10 μg/ml) reversed resistance in RPMI-8226/TP-110 cells (Table 5). Furthermore, K-562/DOX cells expressing ABCB1 also showed strong resistance to TP-110 as compared to MG-132 and bortezomib (Table 6). This suggests that RPMI-8226/TP-110 cells expressing ABCB1 (MDR1) are incidentally isolated in the exposure of TP-110 to RPMI-8226 cells, and acquire cross-resistance to antitumor drugs. K-562/DOX show similar cross-resistance to TP-110 and doxorubicin, suggesting that TP-110 is effluxed by the same mechanism as doxorubicin. Neither the RPMI-8226/TP-110 cells nor the K-562/DOX cells

Table 3. Gene Expression Changes in RPMI-8226/TP-110 Cells

Increased expression of mRNA in RPMI-8226/TP-110		
Gene name	Gene symbol	$\log_2$ of expression ratio
ATP-binding cassette, sub-family B (MDR/TAP), member 1	*ABCB1*	5.89
Hypothetical protein FLJ10178	*FLJ10178*	5.82
Heat shock 22 kDa protein 8	*HSPB8*	5.34
Chemokine (C-C motif) ligand 2	*CCL2*	5.28
Autism susceptibility candidate 2	*AUTS2*	4.97
Rap2 binding protein 9	*RPIB9*	4.87
Zinc finger protein 521	*ZNF521*	4.82
Cytochrome P450, family 24, subfamily A, polypeptide 1	*CYP24A1*	4.72
Crypto	*CFC1*	4.41
BTB (POZ) domain containing 3	*BTBD3*	4.37
Decreased expression of mRNA in RPMI-8226/TP-110		
Gene name	Gene symbol	$\log_2$ of expression ratio
Fibronectin 1, transcript variant 1	*FN1*	−6.17
Soluble carrier family 27 (fatty acid transporter), member 2	*SLC27A2*	−5.79
Target of myb1-like 1 (chicken)	*TOM1L1*	−5.66
Ependymin related protein 1 (zebrafish)	*EPDR1*	−5.47
Ca^{2+}-dependent activator protein for secretion 2	*CADPS2*	−5.37
KIAA0802	*KIAA0802*	−5.09
STARD3 N-terminal like	*STARD3NL*	−5.04
High mobility group AT-hook2	*HMGA2*	−4.92
Hypotherical protein FLJ14564	*FLJ14564*	−4.91
Doublesex and meb-3 related transcription factor 2	*DMRT2*	−4.85

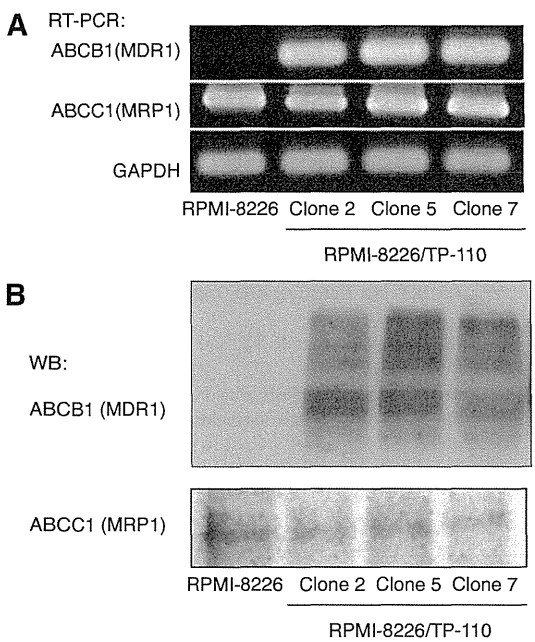

Fig. 4. Expression of ABCB1 and ABCC1 in RPMI-8226/TP-110 Cells.

RPMI-8226 and RPMI-8226/TP-110 cells were incubated for 24 h. A, *ABCB1* and *ABCC1* mRNA expression was assessed by RT-PCR. B, ABCB1 and ABCC1 protein expression was assessed by Western blot analysis.

were resistant to lactacystin. This susceptibility depends on the physico-chemical properties of the compound, including its hydrophobicity and molecular weight.[21,22]

Resistance to chemotherapeutic agents is a significant problem in the treatment of cancer.[14] Colchicine, doxorubicin, etoposide, vinblastin, and paclitaxel are frequently effluxed by P-gp in resistant tumor cells. RPMI-8226/TP-110 cells expressing ABCB1 (MDR1) are incidentally isolated by the exposure of RPMI-8226 cells to TP-110, though their cells do not express ABCC1 (MRP1) (Table 4), and thus RPMI-8226/TP-110 cells show cross-resistance to various anti-tumor drugs. Accordingly, TP-110 exhibits potent anti-tumor activity *in vitro* but continuous administration of TP-110 to mice is assumed to induce expression of P-gp.

On DNA microarray analysis, 44 ABC transporters were investigated. As shown in Table 4, *ABCB1* was strongly overexpressed and *ABCG1* was slightly overexpressed in RPMI-8226/TP-110 cells. Conversely, *ABCG8* was repressed in the RPMI-8226/TP-110 cells. *ABCG1* is reported to regulate the functions of macrophage cholesterol and phospholipid transport in Drosophila,[18] but the functions of these genes in humans are not known.

Drug resistance can be avoided by inhibiting the function of transporters induced by chemotherapy. Verapamil in breast cancer and non-small cell lung carcinoma and cyclosporin A in acute myeloid leukemia have shown benefits in clinical trials.[23] A third generation of inhibitors, including PSC833 and MS-209, are now being developed.[19] Therefore, combination therapy with TP-110 and an ABCB1 inhibitor might produce beneficial effects *in vivo*.

Inconsistent findings involving proteasome inhibitors and P-gp have been reported. Bortezomib and MG-132, proteasome inhibitors, reportedly reduced the degree of the MDR in MCF-7/DOX cells,[24] and MG-132 apparently reversed the MDR of gastric cancer by inhibiting P-gp.[25] These findings suggest that proteasome inhibitors attenuate the expression of P-gp and induce

Table 4. Expression of ABC Transporter Genes in RPMI-8226/TP-110 Cells

Gene symbol	Sub-family	$\log_2$ of expression ratio
ABCA1	ABC1	−0.19
ABCA2	ABC1	0.52
ABCA4	ABC1	0.00
ABCA5	ABC1	0.06
ABCA6	ABC1	−0.24
ABCA7	ABC1	−0.28
ABCA8	ABC1	0.00
ABCA9	ABC1	0.53
ABCA10	ABC1	−0.18
ABCA12	ABC1	0.39
ABCB1	MDR/TAP	5.89
TAP1	MDR/TAP	0.50
TAP2	MDR/TAP	0.45
ABCB4	MDR/TAP	0.59
ABCB5	MDR/TAP	0.00
ABCB6	MDR/TAP	−0.04
ABCB7	MDR/TAP	0.13
ABCB8	MDR/TAP	0.39
ABCB9	MDR/TAP	−0.05
ABCB10	MDR/TAP	0.06
ABCB11	MDR/TAP	0.19
ABCC1	CFTR/MRP	−0.31
ABCC2	CFTR/MRP	1.09
ABCC3	CFTR/MRP	0.11
ABCC4	CFTR/MRP	−0.44
ABCC5	CFTR/MRP	0.71
ABCC6	CFTR/MRP	−0.26
CFTR	CFTR/MRP	−0.22
ABCC8	CFTR/MRP	0.47
ABCC9	CFTR/MRP	0.80
ABCC10	CFTR/MRP	0.73
ABCC11	CFTR/MRP	−0.36
ABCC12	CFTR/MRP	0.00
ABCC13	CFTR/MRP	0.00
ABCD2	ALD	0.36
ABCD3	ALD	−0.01
ABCE1	OABP	−0.34
ABCF1	GCN20	0.57
ABCF2	GCN20	0.14
ABCG1	WHITE	1.92
ABCG2	WHITE	−0.55
ABCG4	WHITE	0.59
ABCG5	WHITE	0.00
ABCG8	WHITE	−3.02

Table 5. Effects of Verapamil on RPMI-8226/TP-110 Cells

Verapamil (10 μg/ml)	IC_{50} (μg/ml)			
	RPMI-8226		RPMI-8226/TP-110 clone 5	
	−	+	−	+
TP-110	0.030	0.028	0.37 (12.3*)	0.053 (1.8)
MG-132	0.50	0.28	1.9 (3.8)	0.48 (0.96)
Bortezomib	0.0019	0.0019	0.0030 (1.6)	0.0019 (1.0)
Doxorubicin	0.0037	0.014	1.1 (297)	0.11 (30)

*Values in parentheses indicate index of resistance (fold).

apoptosis in resistant tumor cells. On the other hand, the proteasome inhibitors bortezomib and MLN273 are substrates of P-gp in leukemic cells, and knockdown of P-gp resensitizes cells against these inhibitors.[26] Ohkawa *et al.* reported a possible role of calpain in P-gp turnover.[27] In the RPMI-8226/TP-110 cells, our results clearly indicate that a proteasome inhibitor, TP-110, is the substrate of ABCB1 (P-gp).

Table 6. Effects of TP-110 on Doxorubicin-Resistant K-562/DOX Cells

	IC_{50} (μg/ml)	
	K-562	K-562/DOX
TP-110	0.053	4.8 (91*)
MG-132	1.6	5.1 (3.0)
Bortezomib	0.0093	0.037 (4.0)
Lactacystin	0.44	0.40 (0.90)
Doxorubicin	0.046	2.8 (60)

*Values in parentheses indicate index of resistance (fold).

In conclusion, results of the present study indicate that the resistance factor in established RPMI-8226/TP-110 cells is *ABCB1*. Overexpression of ABCB1 in the RPMI-8226/TP-110 cells was indicated by the results of DNA microarray analysis, and was supported by the results of RT-PCR and Western blotting. Moreover, the addition of an ABCB1 inhibitor, verapamil, reversed resistance in the RPMI-8226/TP-110 cells. These results suggest that TP-110 therapy requires such inhibitors to overcome resistance *via* P-gp. Chemical modification of TP-110 and/or combination therapy with an ABCB1 inhibitor is a promising approach in cancer chemotherapy.

Acknowledgment

This work was supported by the Ministry of Health, Labor, and Welfare of Japan as part of the Third-Term Comprehensive Ten Year Strategy for Cancer Control.

References

1) Adams J, *Nat. Rev. Cancer*, **4**, 349–360 (2004).
2) Chauhan D, Hideshima T, and Anderson KC, *Annu. Rev. Pharmacol. Toxicol.*, **45**, 465–476 (2005).
3) Almond JB and Cohen GM, *Leukemia*, **16**, 433–443 (2002).
4) Adams J, Behnke M, Chen S, Cruickshank AA, Dick LR, Grenier L, Klunder JM, Ma YT, Plamondon L, and Stein RL, *Bioorg. Med. Chem. Lett.*, **8**, 333–338 (1998).
5) Orlowski RZ and Kuhn DJ, *Clin. Cancer Res.*, **14**, 1649–1657 (2008).
6) Kane RC, Bross PF, Farrell AT, and Pazdur R, *Oncologist*, **8**, 508–513 (2003).
7) Momose I, Sekizawa R, Hashizume H, Kinoshita N, Homma Y, Hamada M, Iinuma H, and Takeuchi T, *J. Antibiot.*, **54**, 997–1003 (2001).
8) Momose I, Sekizawa R, Hirosawa S, Ikeda D, Naganawa H, Iinuma H, and Takeuchi T, *J. Antibiot.*, **54**, 1004–1012 (2001).
9) Momose I, Sekizawa R, Iinuma H, and Takeuchi T, *Biosci. Biotecnol. Biochem.*, **66**, 2256–2258 (2002).
10) Momose I, Umezawa Y, Hirosawa S, Iinuma H, and Ikeda D, *Bioorg. Med. Chem. Lett.*, **15**, 1867–1871 (2005).
11) Momose I, Umezawa Y, Hirosawa S, Iijima M, Iinuma H, and Ikeda D, *Biosci. Biotechnol. Biochem.*, **69**, 1733–1742 (2005).
12) Momose I, Iijima M, Kawada M, and Ikeda D, *Biosci. Biotechnol. Biochem.*, **71**, 1036–1043 (2007).
13) Iijima M, Momose I, and Ikeda D, *Anticancer Res.*, **29**, 977–985 (2009).
14) Tsuruo T, Naito M, Tomida A, Fujita N, Mashima T, Sakamoto H, and Haga N, *Cancer Sci.*, **94**, 15–21 (2003).
15) Dean M, Fojo T, and Bates S, *Nat. Rev. Cancer*, **5**, 275–284 (2005).
16) Cole SP, Bhardwaj G, Gerlach JH, Mackie JE, Grant CE, Almquist KC, Stewart AJ, Kurz EU, Duncan AM, and Deeley RG, *Science*, **258**, 1650–1654 (1992).
17) Doyle LA, Yang W, Abruzzo LV, Krogmann T, Gao Y, Rishi AK, and Ross DD, *Proc. Natl. Acad. Sci.*, **95**, 15665–15670 (1998).

18) Belpomme D, Gauthier S, Pujade-Lauraine E, Facchini T, Goudier MJ, Krakowski I, Netter-Pinon G, Frenay M, Gousset C, Marié FN, Benmiloud M, and Sturtz F, *Ann. Oncol.*, **11**, 1471–1476 (2000).
19) Greenberg PL, Lee SJ, Advani R, Tallman MS, Sikic BI, Letendre L, Dugan K, Lum B, Chin DL, Dewald G, Paietta E, Bennett JM, and Rowe JM, *J. Clin. Oncol.*, **22**, 1078–1086 (2004).
20) Dreicer R, Petrylak D, Agus D, Webb I, and Roth B, *Clin. Cancer Res.*, **13**, 1208–1215 (2007).
21) Tang-Wai DF, Brossi A, Arnold LD, and Gros P, *Biochemistry*, **32**, 6470–6476 (1993).
22) Ueda K, Okamura N, Hirai M, Tanigawara Y, Saeki T, Kioka N, Komano T, and Hori R, *J. Biol. Chem.*, **267**, 24248–24252 (1992).
23) Klucken J, Buchler C, Orso E, Kaminski WE, Porsch-Ozcurumez M, Liebisch G, Kapinsky M, Diederich W, Drobnik W, Dean M, Allikmets R, and Schmitz G, *Proc. Nat. Acad. Sci.*, **97**, 817–822 (2000).
24) Fujita T, Washio K, Takabatake D, Takahashi H, Yoshitomi S, Tsukuda K, Ishibe Y, Ogasawara Y, Doihara H, and Shimizu N, *Int. J. Cancer*, **117**, 670–682 (2005).
25) Zhang Y, Shi Y, Li X, Du R, Luo G, Xia L, Du W, Chen B, Zhai H, Wu K, and Fan D, *Cancer Biol. Ther.*, **7**, 540–546 (2008).
26) Rumpold H, Salvador C, Wolf AM, Tilg H, Gastl G, and Wolf D, *Biochem. Biophys. Res. Commun.*, **361**, 549–554 (2007).
27) Ohkawa K, Asakura T, Takada K, Sawai T, Hashizume Y, Okawa Y, and Yanaihara N, *Int. J. Oncol.*, **15**, 677–686 (1999).

Bioorganic & Medicinal Chemistry Letters 20 (2010) 5839–5842

Contents lists available at ScienceDirect

Bioorganic & Medicinal Chemistry Letters

journal homepage: www.elsevier.com/locate/bmcl

Structure–activity relationship of boronic acid derivatives of tyropeptin: Proteasome inhibitors

Takumi Watanabe [a,*], Hikaru Abe [a], Isao Momose [b], Yoshikazu Takahashi [a], Daishiro Ikeda [b], Yuzuru Akamatsu [a]

[a] Institute of Microbial Chemistry, Tokyo, 3-14-23 Kamiosaki, Shinagawa-ku, Tokyo 141-0021, Japan
[b] Institute of Microbial Chemistry, Numazu, 18-24 Miyamoto, Numazu 410-0301, Japan

ARTICLE INFO

Article history:
Received 20 July 2010
Revised 26 July 2010
Accepted 27 July 2010
Available online 1 August 2010

Keywords:
Proteasome inhibitor
Boronic acid
Structure–activity relationship
Cytotoxicity
Multiple myeloma
Tyropeptin

ABSTRACT

The structure–activity relationship of the boronic acid derivatives of tyropeptin, a proteasome inhibitor, was studied. Based on the structure of a previously reported boronate analog of tyropeptin (**2**), 41 derivatives, which have varying substructure at the N-terminal acyl moiety and P2 position, were synthesized. Among them, 3-phenoxyphenylacetamide **6** and 3-fluoro picolinamide **22** displayed the most potent inhibitory activity toward chymotryptic activity of proteasome and cytotoxicity, respectively. The replacement of the isopropyl group in the P2 side chain to H or Me had negligible effects on the biological activities examined in this study.

Proteasome, a multicatalytic threonine protease, is responsible for ubiquitin-dependent nonlysosomal proteolysis.[1] This enzyme has three distinct active sites that are individually responsible for the chymotrypsin-like, caspase-like, and trypsin-like proteolytic activities.[2] Among these, the chymotrypsin-like activity is of greatest interest, and much research in medicinal chemistry has been focused on it.[3,4]

Elevated levels of the proteasome have been implicated in many diseases including cancer. In fact, it has been reported that the anti-cancer activity of proteasome inhibitors is due to inhibition of the transcriptional factor NF-κB;[5,6] stabilization of p21, p27, and p53;[7,8] and suppression of the unfolded protein response (UPR).[9] Indeed, proteasome inhibitors have been recognized as promising candidates for anti-cancer agent,[10,11] since the US Food and Drug Administration approved the first clinical use of a compound from this class, bortezomib **3** (also referred to as PS-341, Velcade®), for the treatment of multiple myeloma.

Previously, we reported the isolation and structural determination of the novel proteasome inhibitors tyropeptins A (**1**) produced by *Kitasatospora sp.* MK993-dF2,[12,13] and structure–activity relationship (SAR) studies of tyropeptin derivatives.[14,15] In these studies, tyropeptin-boronic acid derivatives (**2** as a representative) were found to exhibit enhanced inhibitory activity against chymotrypsin-like activity of human proteasome when compared to tyropeptin A (Fig. 1).

Encouraged by these results, we conducted further SAR studies of tyropeptin-boronic acid derivatives. In the present study, the effect of acyl moiety located at the N-terminus on the proteasome-inhibitory activity and cytotoxicity against RPMI8226 cells derived from multiple myeloma was investigated. Proteasome-inhibitory activities were determined using purified human erythrocyte-derived 20S proteasome (Enzo Life Sciences. Plymouth Meeting, PA) as previously described.[13]

Scheme 1 summarizes the procedure for synthesizing the tyropeptin-boronic acid derivatives used in this study. According to the method reported previously,[15] 41 analogs of **2** that have a variety of acyl groups at the N-terminus were prepared using WSC·HCl as a coupling reagent with corresponding carboxylic acids and the peptide boronate **4**.[16]

Table 1 shows the inhibitory activity toward proteasome and the cytotoxicity of tyropeptin-boronic acid derivatives synthesized for this study. The almost identical biological activities were observed for the previously reported 1-naphtylacetyl derivative **2** and its regioisomer **5**. The most potent inhibitor of chymotrypsin-like activity was analog **6**, which has a 3-phenoxyphenylacetyl group at the N-terminal acyl moiety; almost ninefold more potent than bortezomib **3** (IC_{50}: 0.0041 for **6** and 0.039 μM for **3**). Unfortunately these compounds showed weak antitumor activity,[17] which prompted us to use different acyl groups. Instead, we chose

* Corresponding author. Tel.: +81 3 3441 4173; fax: +81 3 3441 7589.
E-mail address: twatanabe@bikaken.or.jp (T. Watanabe).

0960-894X/$ - see front matter © 2010 Elsevier Ltd. All rights reserved.
doi:10.1016/j.bmcl.2010.07.122

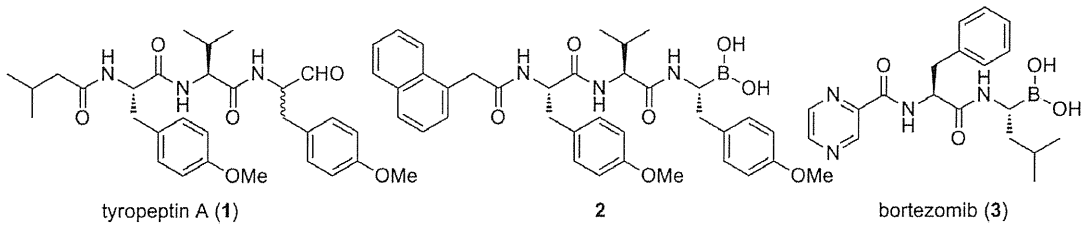

Figure 1. Structure of tyropeptin A (**1**), a tyropeptin-boronic acid derivative (**2**), and bortezomib (**3**).

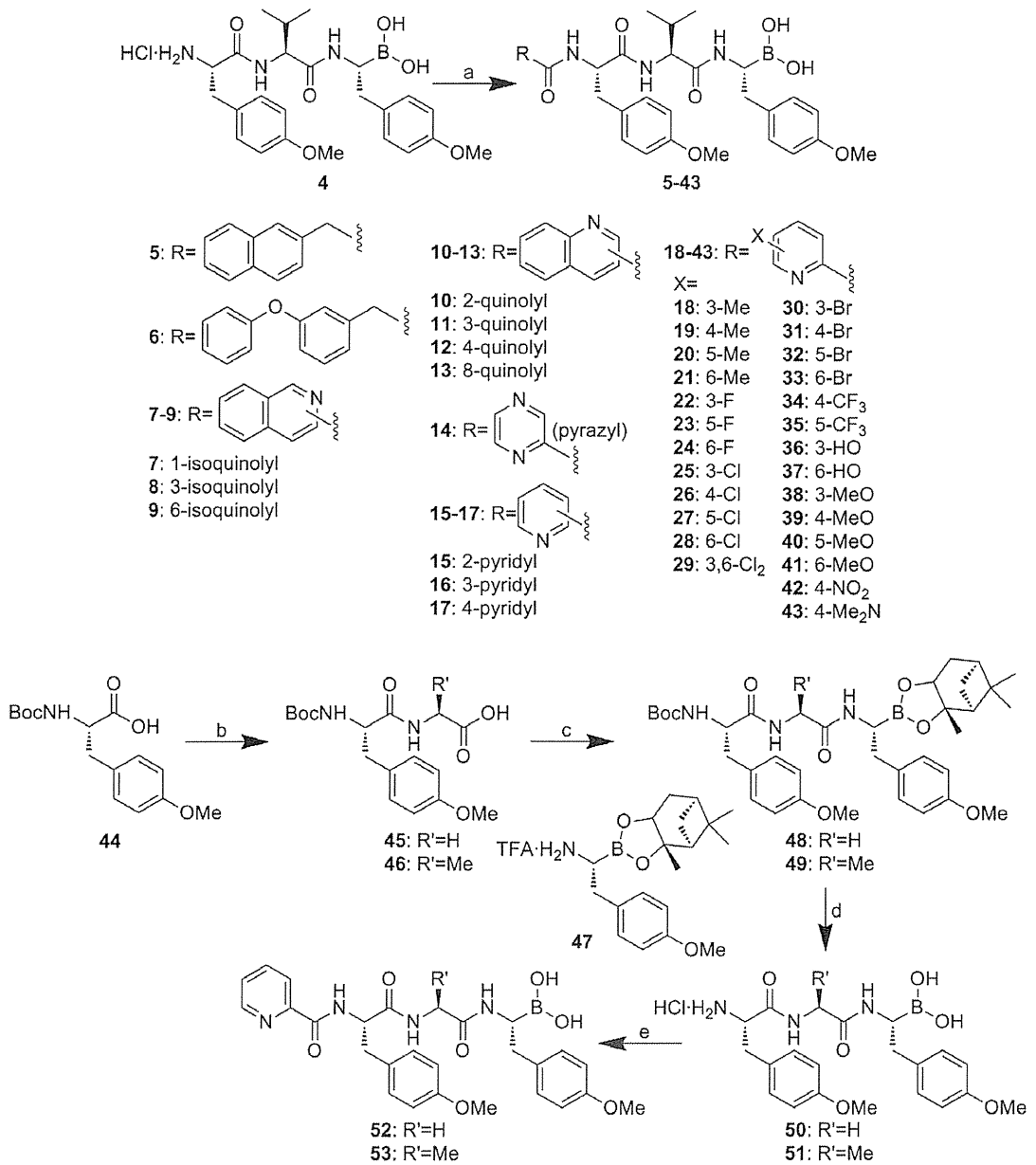

Scheme 1. Reagents and conditions: (a) carboxylic acid, WSC·HCl, HOBt, iPr$_2$NEt, CH_2Cl_2; (b) (i) H-Gly-OBn or H-Ala-OBn, WSC·HCl, HOBt, iPr$_2$NEt, CH_2Cl_2; (ii) H_2, Pd/C, MeOH; (c) **47**, WSC·HCl, HOBt, iPr$_2$NEt, CH_2Cl_2; (d) (i) TFA, $CHCl_3$; (ii) iBuB(OH)$_2$, 1 M HCl, hexane; (e) 2-picolinic acid, WSC·HCl, HOBt, iPr$_2$NEt, CH_2Cl_2.

various N-heteroaromatic rings because bortezomib **3** has a pyrazine carboxamide moiety.

First, amide derivatives of commercially available carboxylic acids having quinoline, isoquinoline, pyrazine, and pyridine nuclei

Table 1
Biological activities of tyropeptin-boronic acid derivatives, and bortezomib (IC_{50}: μM)

Compounds	Chymotrypsin-like activity	Caspase-like activity	Trypsin-like activity	Cytotoxicity (RPMI8226)
5	0.022	39	12	0.17
6	0.0041	29	1.1	0.19
7	0.041	19	10	0.034
8	0.059	11	9	0.093
9	0.38	>40	>40	0.26
10	0.10	16	5.4	0.073
11	0.056	32	10	0.054
12	0.049	24	8.6	0.049
13	0.093	16	18	0.056
14	0.24	33	19	0.017
15	0.23	23	40	0.013
16	0.50	>40	>40	0.87
17	2.3	>40	>40	0.87
18	0.085	>40	20	0.014
19	0.14	30	20	0.014
20	0.12	30	14	0.014
21	0.088	30	17	0.014
22	0.14	25	24	0.0049
23	0.081	30	14	0.019
24	0.11	27	20	0.015
25	0.083	20	20	0.0097
26	0.088	21	15	0.039
27	0.083	16	15	0.039
28	0.10	23	10	0.029
29	0.053	26	13	0.014
30	0.061	20	17	0.013
31	0.095	17	14	0.047
32	0.093	24	14	0.046
33	0.092	27	14	0.044
34	0.15	25	20	0.053
35	0.11	28	19	0.047
36	0.39	29	>40	0.052
37	0.24	>40	11	0.34
38	0.13	26	31	0.041
39	0.087	20	16	0.013
40	0.094	21	14	0.013
41	0.059	35	21	0.051
42	0.19	34	19	0.048
43	0.11	21	15	0.044
52	0.26	34	>40	0.024
53	0.11	>40	>40	0.057
2	0.019	39	>40	0.028
3	0.039	0.75	>40	0.0088

without any substituents were prepared (**7**–**17**). Except for compound **10**, the quinoline and isoquinoline derivatives inhibited the chymotrypsin-like activity of proteasome more effectively than the pyrazine and pyridine congeners. It is noteworthy that inhibition of proteasome did not necessarily correlate with the cytotoxicity. Indeed, the most potent cytotoxicity, comparable to that of bortezomib, was observed for picolinic acid amide **15**, albeit a modest inhibitory activity against proteasome. Because the analog **15** displayed an antitumor activity in a preliminary experiment,[17] further SAR studies were performed starting with this analog to clarify the effects of substituents on the pyridine ring. To this end, various picolinic groups installed with one (or two in the case of 3,6-dichloroderivative **29**) functional group were introduced at the N-terminus (**18**–**43**): Me, F, Cl, Br, CF_3, OH, OMe, NO_2, or NMe_2 derivatives.

In most cases, when tested against the chymotrypsin-like activity of proteasome, analogs with additional substituents showed IC_{50} values lower than that of **15** (0.23 μM) except for hydroxylated derivatives **36** and **37** (IC_{50}: 0.39 and 0.24 μM, respectively). In particular, the 3,6-Cl_2 (**29**), 3-Br (**30**), and 6-Me (**41**) derivatives showed comparable potency (IC_{50}: 0.053, 0.061, and 0.059 μM, respectively) to that of bortezomib **3**.

Substantial loss of cytotoxicity toward RPMI8226 was not observed for the compounds of this class. Notably, 3-F derivative **22** displayed one of the most potent cytotoxicities against RPMI8226 among the tyropeptin-related compounds synthesized in our laboratory (IC_{50}: 0.0049 μM). Here again, the potency of the inhibitory activity toward proteasome and cytotoxicity did not coincide with each other. In fact, **22** showed only a moderate activity toward proteasome (IC_{50}: 0.14 μM).

Other than the deleterious effect of an OH group on the inhibition of chymotryptic activity, no obvious relationship was observed between the biological activities examined in this study and the structure of the pyridyl moiety.

In addition, a preliminary study to evaluate the effect of the P2 side chain was conducted. Based on the structure of **15**, two analogs, in which the P2 valine was replaced with either glycine (**52**) or alanine (**53**), were prepared using a procedure that was analogous to the synthesis of the above-mentioned tyropeptin derivatives. As a result, removal of all or part of the P2 side chain of **15** did not influence the biological activity tested in this study.[16]

In summary, boronic acid derivatives of tyropeptin were synthesized and tested for proteasome-inhibitory activity and cytotoxicity against RPMI8226 in this study. The most potent compounds found were 3-phenoxyphenylaceamide **6** (for proteasome-inhibitory activity) and 3-fluoropicolinamide **22** (for cytotoxicity). The structural change in P2 did not affect the in vitro activities tested in this study. In order to clarify whether the structural change of P2 side chain can alter the physicochemical properties of analogs without affecting the biological activities, a SAR study on this moiety is currently under way. Moreover, full details of the antitumor activities of these compounds will be also reported in due course.

Acknowledgments

The authors thank Dr. Ryuich Sawa and Ms. Yumiko Kubota at Institute of Microbial Chemistry, Tokyo, for collecting analytical data. The authors are also grateful to Ms. Shoko Kakuda at Institute of Microbial Chemistry, Numazu, for evaluation of biological activity.

References and notes

1. Ciechanover, A. *Angew. Chem., Int. Ed.* **2005**, *44*, 5944.
2. Kisselev, A. F.; Goldberg, A. L. *Methods Enzymol.* **2005**, *398*, 364.
3. Lopes, U. G.; Erhardt, P.; Yao, R.; Cooper, G. M. *J. Biol. Chem.* **1997**, *272*, 12893.
4. An, B.; Goldfarb, R. H.; Siman, R.; Dou, Q. P. *Cell Death Differ.* **1998**, *5*, 1062.
5. Frankel, A.; Man, S.; Elliot, P.; Adams, J.; Kerbel, R. S. *Clin. Cancer Res.* **2000**, *6*, 33719.
6. Sunwoo, J. B.; Chen, Z.; Dong, G.; Yeh, N.; Bancroft, C. C.; Sausville, E.; Adams, J.; Elliot, P.; Van Waes, C. *Clin. Cancer Res.* **2001**, *7*, 1419.
7. Hideshima, T.; Richardson, P.; Chauhau, D.; Palombella, V. J.; Elliot, P. J.; Adams, J.; Anderson, K. C. *Cancer Res.* **2001**, *61*, 3071.
8. Ling, Y.-H.; Liebes, L.; Jiang, J.-D.; Holland, J. F.; Elliot, P. J.; Adams, J.; Muggia, F. M.; Perez-Solar, R. *Clin. Cancer Res.* **2003**, *9*, 1145.
9. Lee, A.-H.; Iwakoshi, N. N.; Anderson, K. C.; Glimcher, L. H. *Proc. Natl. Acad. Sci. U.S.A.* **2003**, *100*, 9946.
10. Sterz, J.; von Metzler, I.; Hahne, J.-C.; Lamottke, B.; Rademacher, J.; Heider, U. *Expert Opin. Invest. Drugs* **2008**, *17*, 879.
11. Yang, H.; Zonder, J. A.; Dou, P. *Expert Opin. Invest. Drugs* **2009**, *18*, 957.
12. Momose, I.; Sekizawa, R.; Hashizume, H.; Kinoshita, N.; Homma, Y.; Hamada, M.; Iinuma, H.; Takeuchi, T. *J. Antibiot.* **2001**, *54*, 997.
13. Momose, I.; Sekizawa, R.; Hirosawa, S.; Ikeda, D.; Naganawa, H.; Iinuma, H.; Takeuchi, T. *J. Antibiot.* **2001**, *54*, 1004.
14. Momose, I.; Umezawa, Y.; Hirosawa, S.; Iinuma, H.; Ikeda, D. *Bioorg. Med. Chem. Lett.* **2005**, *15*, 1867.
15. Watanabe, T.; Momose, I.; Abe, M.; Abe, H.; Sawa, R.; Umezawa, Y.; Ikeda, D.; Takahashi, Y.; Akamatsu, Y. *Bioorg. Med. Chem. Lett.* **2009**, *19*, 2343.
16. All the new compounds showed satisfactory analytical data. The representatives are listed below: **6**: a white powder: mp 102–105 °C; $[\alpha]_D^{20}$ −36.2 (*c* 0.150, $CHCl_3$); IR (KBr) ν_{max} 3294, 1643, 1512, 1250, 1034 cm^{-1}; ^1H NMR (CD_3OD, 600 MHz); δ 7.32 (2H, m), 7.20 (1H, t, *J* = 7.9 Hz), 7.12 (2H, d, *J* = 8.6 Hz), 7.08 (1H, m), 7.06 (2H, d, *J* = 8.6 Hz), 6.94 (2H, d, *J* = 7.9 Hz), 6.87–6.80 (5H, m), 6.75 (2H, d, *J* = 8.6 Hz), 4.62 (1H, m), 4.31 (1H, d, *J* = 7.6 Hz), 3.73 (3H, s), 3.71 (3H, s), 3.40 (2H, d, *J* = 14.4 Hz), 3.02 (1H, dd, *J* = 14.1, 5.1 Hz), 2.82–2.74 (2H, m), 2.51 (1H, dd, *J* = 14.1, 10.0 Hz), 2.07 (1H, m), 0.95–0.92 (6H, m); ^{13}C NMR (CD_3OD, 150 MHz); δ 177.8, 173.8, 173.5, 160.0, 159.7, 158.8,

158.7, 138.6, 133.8, 131.3, 130.91, 130.88, 130.0, 125.1, 124.4, 120.7, 119.9, 118.2, 115.0, 114.9, 56.5, 55.8, 55.70, 55.65, 43.4, 37.8, 37.3, 31.9, 19.4, 18.8; HRMS (ESI-Orbitrap) *m/z* calcd for $C_{38}H_{44}BN_3NaO_8^+$ [(M+Na)$^+$] 704.3114, found: 704.3096. Compound **15**: a white powder: mp 123–125 °C; $[\alpha]_D^{20}$ −48.0 (*c* 0.260, $CHCl_3$); IR (KBr) ν_{max} 3305, 1658, 1512, 1246, 1176, 1034 cm^{-1}; ^{1}H NMR (CD_3OD, 600 MHz); δ 8.60 (1H, m), 8.00 (1H, m), 7.92 (1H, dt, *J* = 7.7, 1.8 Hz), 7.53 (1H, m), 7.16–7.13 (4H, m), 6.85 (2H, d, *J* = 8.7 Hz), 6.78 (2H, d, *J* = 8.7 Hz), 4.36 (1H, d, *J* = 8.0 Hz), 3.74 (3H, s), 3.71 (3H, s), 3.16 (1H, dd, *J* = 13.9, 5.2 Hz), 2.98 (1H, dd, *J* = 13.9, 8.5 Hz), 2.90 (1H, m), 2.84 (1H, dd, *J* = 14.2, 5.5 Hz), 2.53 (1H, dd, *J* = 14.2, 10.0 Hz), 2.13 (1H, m), 1.00 (3H, d, *J* = 6.2 Hz), 0.99 (3H, d, *J* = 6.2 Hz); ^{13}C NMR (CD_3OD, 150 MHz); δ 177.6, 173.6, 166.1, 160.1, 159.7, 150.4, 149.8, 138.8, 133.8, 131.4, 130.8, 129.7, 128.0, 123.1, 115.0, 114.9, 56.6, 55.9, 55.7, 55.6, 38.4, 37.2, 31.9, 19.4, 18.9; HRMS (ESI-TOF) *m/z* calcd for $C_{30}H_{37}BN_4NaO_7^+$ [(M+Na)$^+$] 599.2648, found: 599.2639. Compound **22**: a white powder: mp 126–128 °C; $[\alpha]_D^{20}$ −39.8 (*c* 0.215, $CHCl_3$); IR (KBr) ν_{max} 3305, 1658, 1512, 1246, 1176, 1034 cm^{-1}; ^{1}H NMR (CD_3OD, 600 MHz); δ 8.60 (1H, m), 7.74–7.70 (1H, m), 7.64–7.61 (1H, m), 7.17 (2H, d, *J* = 8.6 Hz), 7.09 (2H, d, *J* = 8.6 Hz), 6.83 (2H, d, *J* = 8.6 Hz), 6.71 (2H, d, *J* = 8.6 Hz), 4.36 (1H, d, *J* = 7.2 Hz), 3.74 (3H, s), 3.72 (3H, s), 3.10–3.03 (2H, m), 2.84 (1H, dd, *J* = 8.9, 6.2 Hz), 2.76 (1H, dd, *J* = 14.2, 6.2 Hz), 2.54 (1H, dd, *J* = 14.2, 8.9 Hz), 2.07 (1H, m), 2.13 (1H, m), 0.84 (3H, d, *J* = 6.5 Hz), 0.81 (3H, d, *J* = 6.5 Hz); ^{13}C NMR (CD_3OD, 150 MHz); δ 178.0, 173.7, 164.3 (d, *J* = 5.7 Hz), 160.5 (d, *J* = 268.6 Hz), 160.3, 159.6, 145.9 (d, *J* = 5.7 Hz), 138.6 (d, *J* = 5.7 Hz), 133.9, 131.5, 130.9, 130.1 (d, *J* = 5.7 Hz), 129.6, 127.5 (d, *J* = 20.1 Hz), 115.1, 114.9, 56.9, 56.2, 55.71, 55.69, 38.7, 37.0, 31.1, 19.4, 18.6; HRMS (ESI-Orbitrap) *m/z* calcd for $C_{30}H_{36}BFN_4NaO_7^+$ [(M+Na)$^+$] 617.2553, found: 617.2568.

17. Manuscript in preparation.

American Journal of Nephrology

American Journal of Nephrology

Dendrin location in podocytes is associated with the disease progression in animal and human glomerulopathy

Journal:	*American Journal of Nephrology*
Manuscript ID:	AJNE-2011-Jan-00060.R2
mstype:	Laboratory Investigation
Date Submitted by the Author:	30-Mar-2011
Complete List of Authors:	ASANUMA, KATSUHIKO; Juntendo University, Division of Nephrology Takagi-Akiba, Miyuki; Juntendo University, Division of Nephrology Kodama, Fumiko; Juntendo University, Division of Nephrology Asao, Rin; Juntendo University, Division of Nephrology Nagai, Yoshiko; Juntendo University, Division of Nephrology Lydia, Aida; University of Indonesia, Division of Nephrology and Hypertension Fukuda, Hiromitsu; Juntendo University, Division of Nephrology Tanaka, Eriko; Juntendo University, Division of Nephrology Shibata, Terumi; Juntendo University, Division of Nephrology Takahara, Hisatsugu; Juntendo University, Division of Nephrology Hidaka, Teruo; Juntendo University, Division of Nephrology Asanuma, Etsuko; Juntendo University, Division of Nephrology Kominami, Eiki; Juntendo University, Department of Biochemistry Ueno, Takashi; Juntendo University, Department of Biochemistry Tomino, Yasuhiko; Juntendo University, Division of Nephrology
Keywords:	podocytes, glomerulosclerosis, nephropathy, dendrin, ADR mice

Dendrin location in podocytes is associated with the disease progression in animal and human glomerulopathy

Katsuhiko Asanuma 1,5, Miyuki Akiba-Takagi 1,5, Fumiko Kodama 1, Rin Asao 1, Yoshiko Nagai 1, Aida Lydia 1,2, Hiromitsu Fukuda 1, Eriko Tanaka 1,3, Terumi Shibata 1, Hisatsugu Takahara 1, Teruo Hidaka1, Etsuko Asanuma 1, Eiki Kominami 3, Takashi Ueno 2, Yasuhiko Tomino 1

1, Department of Internal Medicine, Division of Nephrology, Juntendo University Faculty of Medicine, Tokyo, Japan

2, Division of Nephrology and Hypertension, Department of Internal Medicine, Cipto Mangunkusumo Hospital, University of Indonesia, Jakarta, Indonesia

3, Department of Pediatrics, Tokyo Medical and Dental University, Tokyo, Japan

4, Department of Biochemistry, Juntendo University Faculty of Medicine, Tokyo, Japan

5, K.A., M.A.-T. contributed equally to this article

Short title: Nuclear dendrin in in mouse and human glomerulopathy

Correspondence: (Yasuhiko Tomino M.D.) **Division of Nephrology, Department of Internal Medicine, Juntendo University Faculty of Medicine 2-1-1 Hongo, Bunkyo-ku, Tokyo 113-8421, Japan. Tel**: +81-3-3813-3111, **Fax**: +81-3-3813-1183, **e-mail:** yasu@juntendo.ac.jp

Keywords: dendrin, podocyte, ADR mice, glomeruloscrelosis, nephrosis, apoptosis

Number of words: 3448

Conflict of interest statement: *None declared.*

Abstract

Background: ADR nephrosis in mice has been extensively studied and has enabled a greater understanding of the processes underlying the progression of renal injury. Dendrin is a novel component of the slit diaphragm (SD) with proapoptotic signaling properties, and it accumulates in the podocyte nucleus in response to glomerular injury in mice. The present study re-evaluated chronic progressive nephropathy in ADR mice and the localization of dendrin in mice and in human glomerulopathy. **Methods:** To investigate the localization of dendrin, a mouse model for nephrosis and glomerulosclerosis was used, in which ADR was injected once. WT-1 positive cells and apoptotic cells were counted *in vivo and in vitro*. To check the expression of dendrin in ADR mice, immunostaining and western blot were performed. A survey of dendrin staining was performed on human kidney biopsy specimens. **Results:** The injection of ADR induced proteinuria, podocyte loss and glomerulosclerosis. It also caused the relocation of dendrin from the SD to the podocyte nucleus. We demonstrated the location of dendrin to podocyte nuclei in several human glomerulopathy. The mean occurrence of dendrin-positive nucleus per glomerulus increased in several cases of human glomerulopathy. **Conclusions.** These findings suggest that the relocation of dendrin to the podocyte nuclei is useful as a novel marker of podocyte injury in human glomerulopathy.

Introduction

Podocytes are highly specialized, terminally differentiated epithelial cells that do not show characteristic cell division and proliferation [1]. Podocytes serve as the final barrier to urinary protein loss through the special formation and maintenance of foot processes (FPs) and interposed slit diaphragm (SD) [2]. All forms of nephrotic syndrome are characterized by abnormalities in podocytes, including effacement of FPs and/or molecular reorganization of the SD [1-3]. Defects in podocyte structure, function or number can lead to pathologic lesions, known as focal segmental glomerulosclerosis (FSGS) [4-6]. In rat puromycin aminonucleoside (PAN) nephrosis, injured podocytes are manifested by the loss of interdigitating FPs [7][8], detachment from the glomerular basement membrane (GBM), and associated leakiness of the glomerular filter, resulting in proteinuria [6,7]. A reduction in podocyte numbers directly causes proteinuria and leads to glomerulosclerosis [4,9,9-11]. Several groups have shown that apoptosis is a major cause of podocyte loss from the GBM [4], leading to proteinuria and/or glomerulosclerosis in rat PAN nephrosis [6,11] and in human diabetic nephropathy [12] and IgA nephropathy[9,13].

Adriamycin (ADR) nephrosis is well known as a nephrosis and FSGS model in rats [14,15]. An LPS-induced nephrosis model has been established in mice. The model shows transient proteinuria, but no glomerulosclerosis [16]. The first description of ADR including renal injury was in 1998 in mice [17]. Since then, ADR nephrosis in

mice has been extensively studied and has enabled a greater understanding of the processes underlying the progression of renal injury [18]. To elucidate the mechanism of podocyte injury and podocyte loss from the GBM, it is necessary to re-evaluate podocyte apoptosis, podocyte loss and glomerulosclerosis in the ADR mice during a set time course.

Dendrin is a proline-rich protein of unknown function that was originally identified in telencephalic dendrites of sleep-deprived rats [19]. In the brain, two protein variants (81 kDa, 89kDa) have been identified in cytosolic and membranous protein fractions [19]. Recently, dendrin has been seen as a component of the slit diaphragm (SD) complex that relocates to the nucleus of injured podocytes in a murine model of crescentic glomerulonephritis [20]. Also, TGF-β is now known to promote the nuclear translocation of dendrin, and nuclear dendrin is known to amplify TGF-β-induced podocyte apoptosis. Dunner *et al.* reported that dendrin forms a linear pattern on the epithelial side of the glomerular capillary loops, corresponding to the podocytes of normal humans and minimal change disease (MCD) patients [21]. However, nuclear dendrin was not found in the kidneys of patients with MCD.

In the present study, podocyte apoptosis, podocyte loss and glomeruloscrelosis were re-evaluated in a murine model of chronic progressive nephropathy with significant and persistent proteinuria using ADR. Moreover, the localization of dendrin in model mice and in human glomerular diseases was examined.